# Design & Development of a Shallow Water Echo-Sounder for Marine Platforms

Adnan Qaseem, Muhammad Sohail Tahir, Ammar Hassan Asghar, Tayyaba Kokab, Abdul Haq and Shahid Ali



November 28, 2024

# DESIGN & DEVELOPMENT OF A SHALLOW WATER ECHO-SOUNDER FOR MARINE PLATFORMS

Adnan Qaseem
*Center of Excellence*
Islamabad, Pakistan
adnanqaseem@ymail.com

M. Sohail Tahir
*Center of Excellence*
Islamabad, Pakistan
sohail0933@gmail.com

Ammar Hasan Asghar
*Center of Excellence*
Islamabad, Pakistan
ammar.hasan772@gmail.com

Tayyaba Kokab
*Center of Excellence*
Islamabad, Pakistan
tayyabachemist@yahoo.com

Abdul Haq
*Center of Excellence*
Islamabad, Pakistan
abdulhaq002@gmail.com

Shahid Ali
*Center of Excellence*
Islamabad, Pakistan

*Abstract*— Underwater echo-sounders form an integral part of sonar suite for both surface and sub-surface vessels. These systems ensure the safe operations of the fleet by providing real time distance between boat keel and sea bottom. Herein we report the design and development of a shallow water echo-sounder with excellent acoustic parameters for fleet vessels. Peak Transmit voltage response (TVR) of 170 dB, receive voltage sensitivity (RVS) of –187 dBV/μPa and Electrical impedance of 193 Ω were measured for the prototype echo-sounder. Furthermore, the design of this acoustic transducer has the flexibility of tuning the operation frequency by controlling the sensor geometry. This flexibility ensures the control over operational frequencies and customization as per requirement.

*Keywords:* Shallow water Echo-sounder, PZT, Single Beam, acoustic matching layers, hydrography

## I. INTRODUCTION

Early depth measurements were performed by using a line and a lead weight. From 20th century, depth profiling has been performed using acoustic waves, where a signal from a projector is reflected from the seafloor and received onto a hydrophone system, which is sometimes same as the projector. When the sound velocity in the water is known, the acoustic signal's time of flight from the projector to the seafloor and back measures the distance. [1,2] Since the echo sounders measure the time it takes for an acoustic signal to travel to the seafloor and back, the depth, D (unit: m), is given by:

$$D = {}^{tc}/_{2}$$

Where t (unit: s) is the signal's round trip travel time from the projector to the seafloor and back, and c (unit: m/s) is the average sound velocity in the water column.

Single Beam Echosounders (SBE) with broad variety of capabilities are used by naval fleets, cruise liners, cargo ships, fishing trawlers, and even sporting crafts. [3-6] An SBE essentially consists of a transmitting and a receiving part. The signal is a sinusoidal pulse, controlled by a master clock, which is intensified by a power amplifier. The pulse power level is determined by its carrier frequency. Normally, the pulse is fed to the projector terminals through a transformer to step-up the voltage. The projector's acoustic signal travels to the seafloor, reflects from it and returns to the projector where the acoustic signal is converted into an electrical signal.

The input to the processing system is gated in time domain to keep the transmitted signal from being received directly and also to assure the transmitter has stopped ringing down before the received signal arrives. The received signal is passed through a band-pass filter to eliminate noise. The signal is then passed through a time-variable-gain (TVG) circuit before the signal envelope is detected and the signal is displayed on a monitor. Some SBE also permit raw data to be output for processing and display on Man Machine Interface (MMI).

There are no fundamental differences between the design of echo sounder, side scan sonars and the design of a submarine detection sonar. The differences lie only in scale - frequency, range and target size. Because we are dealing only with short-range or vertical transmissions, refraction of sound, which severely limits the performance of long-range antisubmarine sonars, is unimportant and the propagation losses are well described by the general spherical spreading model.

The high amplitude at the front of the echo time history from the seafloor received by an SBE represents the reflection from the seafloor surface by the normal. The straight reflection of the normally incident signal produces the strongest echo, while the backscatter from the seafloor surface, the first characteristic echo return, has a lower echo amplitude and represents the seafloor surface roughness features and some backscatter from the seafloor near surface layers. This part of the echo is associated with the seafloor roughness topography, underneath materials, and attenuation of the acoustic signals in the near seafloor surface parts. A rough seafloor surface or the occurrence of larger grain sizes in the seafloor materials produces a more complex backscattering envelope with a longer duration, while a flat seafloor produces a sharper, higher amplitude and shorter duration echo return. The second echo is usually connected with the hardness features of the seafloor, where rock will produce a higher amplitude echo than sand and mud. [7-9]

The carrier frequency depends on the echo sounder application. The frequency can span from 10 kHz for *deep-water* use to above 500 kHz for *shallow-water* use. Echo sounder resolution is gauged by pulse length and its carrier frequency. The choice of the pulse length, i.e., number of cycles, depends on the expected bottom type. For a hard rocky bottom, a short pulse length is appropriate. For a muddy soft bottom, a longer pulse length is selected in order to transmit enough acoustic power to control the strength of the echo returning from the seafloor. Transmitted power control is another relevant feature of an echo sounder. Echo sounders can normally be tuned in steps from few to several hundred watts. Generally, low power levels are used in shallow water and higher power levels are recommended for deep water ranging.

The boat's motion and position of the sonar projector relative to the environment have an influence on the echo sounder data. Tide and heaved vertical movement of the ship introduce errors in the depth measurement data, which normally are removed by post processing. Similarly, a vessel's rolling and pitching influences measurements, since the projector will become angled toward the seafloor, which can be a problem for narrow beam projectors. Compensation for rolling and pitching is not generally done in case of on SBEs, which otherwise is mandatory for multi-beam sonar due to their narrower beams. Narrow beams, which normally occur at higher frequencies, will more accurately record the seafloor than broader beams obtained at lower frequencies. The resolution is affected by the pulse length, and if two objects are separated by a distance shorter than half the pulse length, they are shown as one object. When their separation is larger than half the pulse length they are shown as two objects.

When the seafloor consists of several layers of materials, as shown in Figure 1, the echo sounder will identify the various individual layers at low frequencies, while only the topmost layer will be identified at high frequencies. [10,11] The top layer can sometimes be a very soft material such as mud or sea grass with a smooth and gradual transition from the water's acoustic impedance to the acoustic impedance of the next layer. These top layers are not always detected by an echo sounder.

Herein we report the design and development of a shallow water echo-sounder with a resonance frequency of 200 ± 10% kHz. The transducer is modelled both analytically and by Finite element technique. The modelled parameters of the active material (PZT sensor) and modeled transducer match well with the developed prototype. The system meets the benchmark criterion of peak TVR, FFVR and Fr for a shallow water echo-sounder.

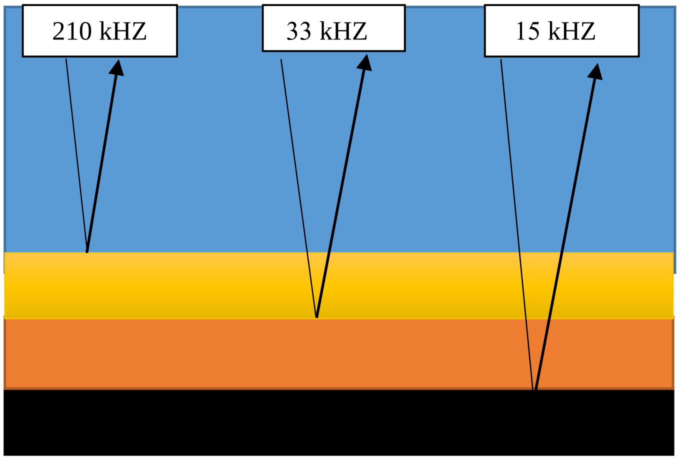


*Figure 1 Layers at sea bottom and effect of lower and higher frequencies ecosounders*

## 1. Methods & Materials

### *1.1 Simulation techniques*

Modelling of the shallow water echo-sunder was done in COMSOL Multiphysics. A 3D geometry of the piezoelectric sensor was created using COMSOL's CAD tools, consisting of a solid PZT-4 ceramic cylinder with a diameter of 41 mm and thickness of 10 mm, a water domain surrounding the ceramic disc to propagate the acoustic waves and a PML (Perfectly Matched Layer) water layer to absorb outgoing waves. [13]

2 D model is depicted in Figure 2. The following physics interfaces were selected and setup to model and simulate the

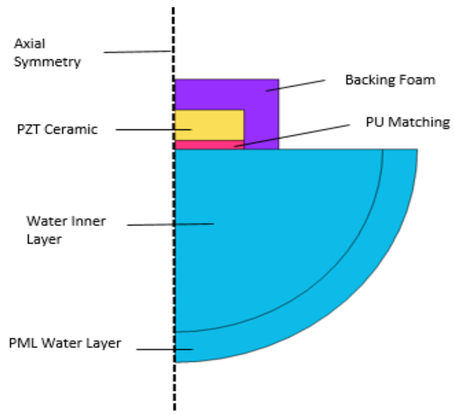


*Figure 2 FEMP Simulation 2D Model: Echosounder with water layers.*

piezoelectric effect in water; Pressure Acoustics Frequency Domain (PAFD), Solid Mechanics (SM), Electrostatics (ES) and Multiphysics Piezoelectric Effect (MPE). Appropriate boundary conditions were applied to the 3D model, including: electric potential and displacement constraints on ceramic cylinder, acoustic pressure and velocity constraints on the water domain and PML boundary conditions on the outer water layer. [14-15]

A free tetrahedral mesh was applied to the 3D geometry, with different mesh sizes used for the solid PZT-4 ceramic and water layers to optimize computational efficiency and accuracy. Maximum number of iterations and mesh refinement was ensured for the effectual simulation. A frequency domain study was setup to analyze the behavior in the frequency range of 170-230 k HZ.

### *1.2 PZT Sensor development*

Prototype sensor was mad by using an indigenously developed high frequency PZT disc. Powder of PZT 4 was compacted into a D2 steel die and compacted to a green density of 65%. The green shape was then thermally treated to remove organic binders and finally sintered at 1250 $^{o}$C for 2 hours to achieve 95% density. The sintered disc was then grinded and lapped to achieve a uniform surface. Silver electrode were screen printed onto both sides of the PZT disc. PZT disc was then fired to achieve good adhesion of silver with PZT surface. The disc was then poled for 30 mins in a silicone oil bath at 105 $^{o}$C at a field of 3kV/mm to polarize the sample. The sample was allowed to age for 10 days and then tested for piezoelectric parameters as per US-Mil-STD 1376. Process flow and equipment used in sensor development is presented in Figure 3.

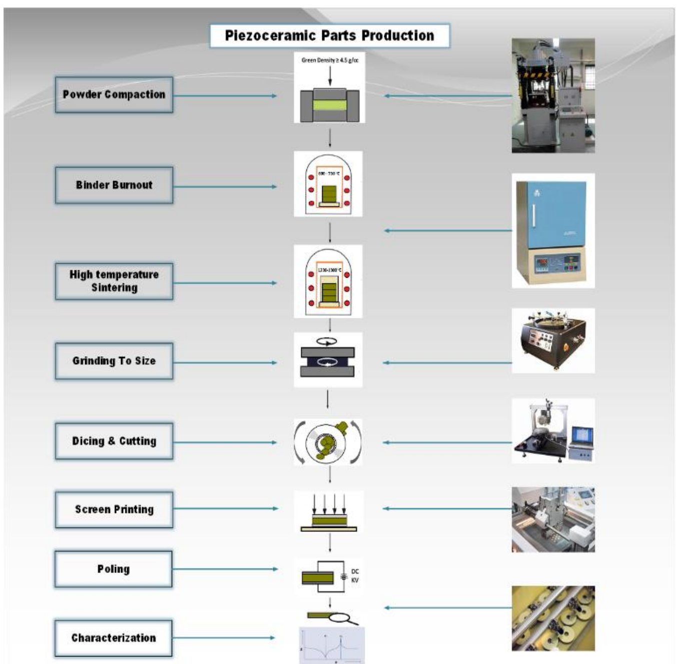


*Figure 3 Process flow of sensor development*

| Thickness | Diameter | Cp | D | $d_{33}$ | Fa | Fr |
|---|---|---|---|---|---|---|
| **mm** | **mm** | **nF** | | **pC/N** | **KHz** | **KHz** |
| 10.2 | 41 | 1.44 | 0.006 | 250 | 217 | 208 |

*Table 1 PZT-4 ceramic disc piezoelectric specifications*

Piezoelectric parameters of the poled disc are given in table 1.

### *1.3 Echo-Sounder Development*

Shallow water echosounder was made using a metallic housing. The PZT disc was placed onto a Polyurethane foam. Connection wires were soldered onto the PZT disc and placed in housing. Acoustically transparent polyurethane was used as acoustic window for sealing the PZT from water and providing good matching with incoming/outgoing acoustic waves.

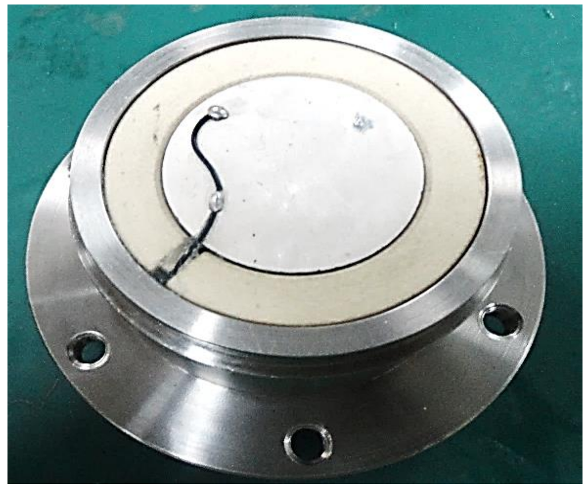

*Figure 4 Echo sounder prototype before molding*

## 2. Results & Discussions:

COMSOL model of the echosounder was prepared by placing the poled PZT ceramic disc onto a porous polyurethane foam backing Figure 5. Porous PU backing allows the block to be air backed and acts as a pressure release material. The pressure release foam has air filled cellular structure. Placing the active element disc on this foam allow maximum transfer of acoustic energy from the transducer to the water body. The foam backed sensor is placed within a metallic housing to prevent corrosion. The front face of the echo sounder is encapsulated with an acoustically transparent polymer jacket with specific acoustic impedance close to that of water. The thickness of this acoustic matching window is chosen on the basis of $\lambda/4$ criterion. The thickness of the acoustic matching layer for this echo sounder was calculated to be 3 mm and the same was used in the fabrication. Quarter wavelength based thickness of the acoustic window minimizes reflections and maximizes the transmission of acoustic energy between the transducer and the water body, improving the overall efficiency and performance of the transducer.

Resonance frequency of a transducer is an important functional parameter signifying the peak transmission point of the transducer. This is indicated by the peaks on the conductance G vs. Frequency F plots (Figure 5). It is noted that three co-existing peaks are simulated on the FEA for our transducer and the same is confirmed on the developed prototype. The alignment of the peaks in both graphs demonstrates the reliability of the COMSOL simulation in predicting the transducer's behavior. This consistency suggests that the simulation model accurately captures the essential physical characteristics of the transducer. The close match between the simulation and test results reinforces the accuracy of the finite element analysis (FEA) conducted in COMSOL. It indicates that the material properties, boundary conditions, and other parameters used in the simulation are well-representative of the actual transducer.

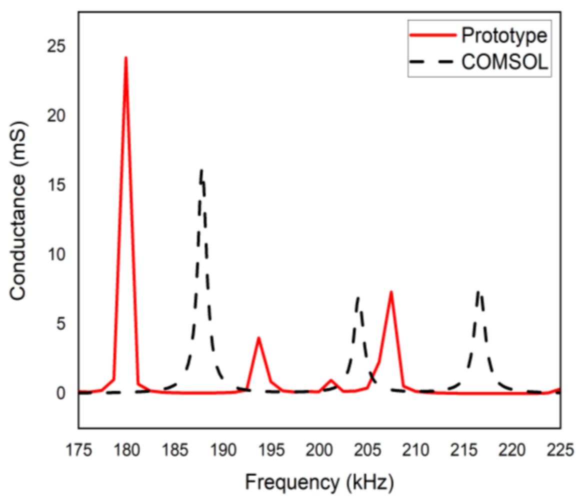


*Figure 5 Conductance plots in air FEA vs. Actual*

Simulating the transducer in water is crucial as it closely replicates the actual operating conditions. The accurate modeling of water properties in FEA ensures that the simulated results are representative of real-world performance.
The simulation identifies the impedance dip at 207.5 kHz (Figure 6), where the impedance reaches its minimum. This frequency represents the optimal operating point for the transducer in water, where it is most efficient at converting electrical signals into acoustic waves. The prototype testing revealed an impedance dip of 211.2 kHz, closely matching the simulated value. This slight deviation of 3.7 kHz (approximately 1.8%), indicating a high degree of accuracy in the simulation. The measured impedance curve also exhibits a clear dip at the resonance frequency, similar to the simulation. Inconsistency in the impedance profile between the simulation and the test results is may be due to the off the shelf material like epoxies and glues used in prototype development. This may also attribute to the unknown parameters like elastic modulus, poison’s ratio and elastic matrix values.
The testing in water provides a realistic assessment of the transducer’s performance. Factors such as the interaction of acoustic waves with the water medium, potential manufacturing variances, and environmental conditions are accounted for, ensuring that the prototype meets the expected performance standards. [17-18]

The acoustic performance of the echo sounder was simulated using COMSOL Multiphysics and subsequently measured on the developed prototype to validate the results. The Finite

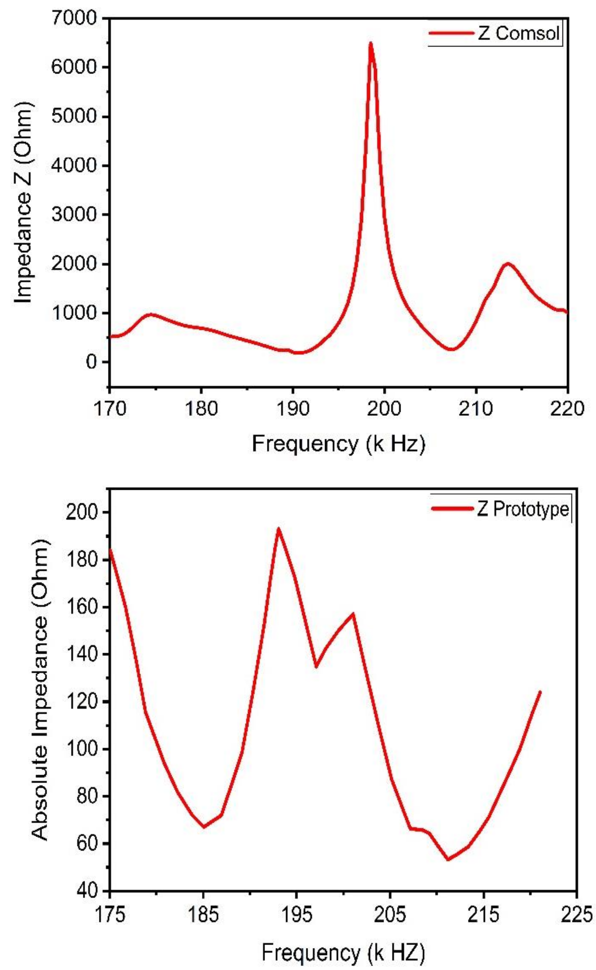


*Figure 6 Impedance plots in water FEA vs. Actual*

Element Analysis (FEA) predicted a peak Transmitting Voltage Response (TVR) of 169 dB at a frequency of 207.5 kHz.
Correspondingly, the measured TVR for the prototype was found to be 170 dB at 211 kHz (Figure 9). This close agreement between the simulated and measured TVR values, with only a 1 dB difference, indicates a high level of accuracy in the simulation model. The slight variation in frequency (3.5 kHz) between the simulation and the prototype is minor, especially given the high frequencies involved, and suggests that the FEA model reliably predicts the transducer’s resonance characteristics. [14]
The excellent correspondence between the FEA simulation and the prototype measurements underscores the reliability of the simulation approach in predicting the acoustic performance of the echo sounder. The small differences observed in both TVR and frequency could be attributed to factors such as material property variations, fabrication tolerances, or environmental conditions. Nonetheless, the simulation’s ability to closely match the actual performance metrics validates its use as an effective tool in the design and optimization of acoustic transducers. This validation is crucial for ensuring that the echo sounder performs as expected in real-world applications, thereby enhancing its operational reliability and efficiency. [17]

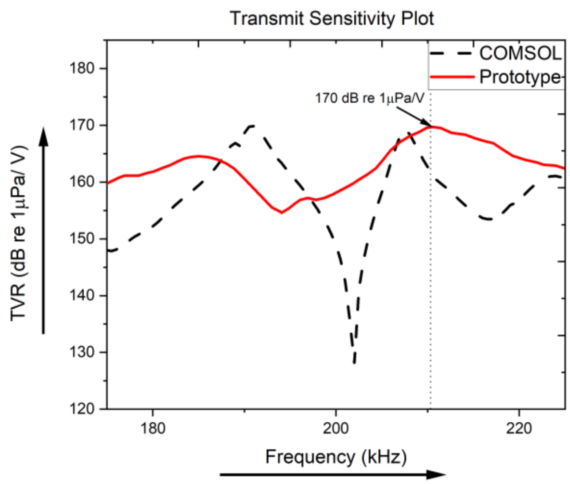


*Figure 7 TVR of simulated and developed echosounder*

Finally, the reception behavior of the echosounder was evaluated both by FE techniques and measured in water tank on the developed prototype (Figure 7). Receive response trend across the frequency of interest followed the simulated trends plots albeit with peak broadening. This can be traced with the inclusion of matching layers and glues that are used in transducer assembly. [18] Receive sensitivity of the transducer was calculated to be -177 dB at 212 kHz against the measured value of -189 dB at the same frequency. This represents a good agreement in terms of peak location between the two results. The difference in RVS at these frequencies is 6% which can be attributed to the viscoelastic encapsulation window materials used in the development of the echo sounder. [12, 18-19]

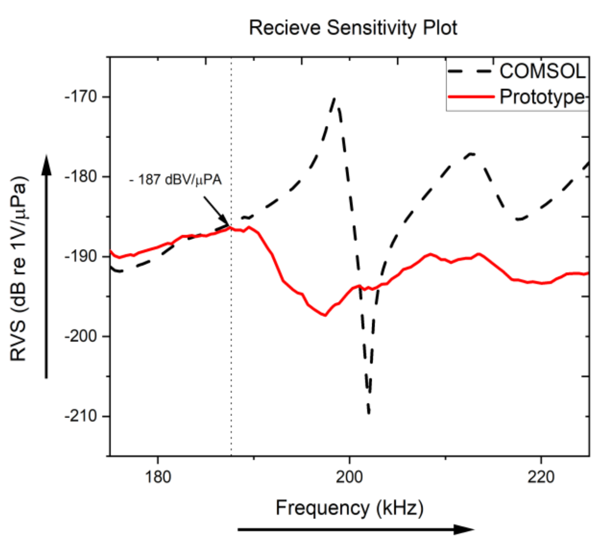


*Figure 7 FFVR of designed and developed echosunder*

## 3. CONCLUSUIONS

This study describes the design and development of a shallow water echosounder with operational frequency of 200 kHz ± 10%. Transducer is designed and modelled by FE techniques in COMSOL multiphysics and this design was validated by fabrication of the prototype. Peak TVR of 169 dB and RVS of -190 dBV/uPa were measured on the developed unit which represents its suitability for shallow water mapping for military and commercial applications. The successful validation of the simulation results by the prototype development instills confidence in the transducer design and manufacturing process. It also highlights areas for potential optimization, such as fine-tuning material properties or manufacturing techniques to further minimize any discrepancies.

### AUTHOR CONTRIBUTIONS

Conceptualization, A.Q. and A.H.; methodology, A.Q. and S.T.; simulation, S.T.; validation, A.Q. and A.H.; formal analysis, S.T.; prototype development, AQ, T.K. and A.H.; investigation, A.Q.; resources, A.H. and S.A.; data curation, A.Q.; writing—original draft preparation, A.Q.; writing—review and editing, A.Q and S.T.; graphs and images A.Q and S.T.; supervision, A.Q. and A.H.; project administration, A.Q. and A.H.; funding acquisition, S.A. All authors have read and agreed to the published version of the manuscript.

### REFERENCES

[1] Irène Mopin, Jacques Marchal, Michel Legris, Gilles Le Chenadec, Philippe Blondel, Benoît Zerr, Design and field testing of a non-linear single-beam echosounder for multi-frequency seabed characterization,Applied Acoustics,Volume 187,2022,108490.

[2] B. R. Biffard, J. M. Preston and N. R. Chapman, "Acoustic Classification with Single-Beam Echosounders: Processing Methods and Theory for Isolating Effects of the Seabed on Echoes," OCEANS 2007, Vancouver, BC, Canada, 2007, pp. 1-8, doi: 10.1109/OCEANS.2007.4449250.

[3] S Pujiyati et al 2020 IOP Conf. Ser.: Earth Environ. Sci. 429 012048

[4] Linløkken, A.N.; Næstad, F.; Langdal, K.; Østbye, K. Comparing Fish Density and Echo Strength Distribution Recorded by Two Generations of Single Beam Echo Sounders. Appl. Sci. 2019, 9, 2041.

[5] Rudstam, Lars G., et al. "Comparison of target strength distributions and fish densities obtained with split and single beam echo sounders." Fisheries Research 42.3 (1999): 207-214.

[6] Becker, J. J., and D. T. Sandwell (2008), Global estimates of seafloor slope from single-beam ship soundings, J. Geophys. Res., 113, C05028, doi:10.1029/2006JC003879.

[7] Flood, Roger D. "Deep-sea sedimentary morphology: modelling and interpretation of echo-sounding profiles." Marine Geology 38.1-3 (1980): 77-92.

[8] Sathishkumar, R., T. V. S. P. Gupta, and M. Ajay Babu. "Echo sounder for seafloor object detection and classification." Journal of Engineering, Computers & Applied Sciences 2.1 (2013): 32.

[9] Smith, D. Taylor, and W. N. Li. "Echo-sounding and sea-floor sediments." Marine geology 4.5 (1966): 353-364.

[10] R. Ferretti, E. Fumagalli, M. Caccia and G. Bruzzone, "Seabed classification using a single beam echosounder," OCEANS 2015 - Genova, Genova, Italy, 2015, pp. 1-5, doi: 10.1109/OCEANS-Genova.2015.7271709.

[11] H. Ni, W. Wang, Q. Ren, L. Lu, J. Wu and L. Ma, "Comparison of Single-beam and Multibeam Sonar Systems for Sediment Characterization: Results from Shallow Water Experiment," OCEANS 2019 MTS/IEEE SEATTLE, Seattle, WA, USA, 2019, pp. 1-4, doi: 10.23919/OCEANS40490.2019.8962802.

[12] C.H. Sherman and J.L. Butler, *Transducers and Arrays for Underwater Sound*, Springer, New York (2007).

[13] Jaffe B, Cook WR, Jaffe H. Piezoelectric ceramics. New York: Academic Press; 1971. p. 142

[14] Becker, E.W., Ehrfeld, W., Hagmann, P., Maner, A. and Munchmeyer, D. (1986), "Fabrication of microstructures with high aspect ratios and great structural heights by synchrotron radiation lithography, galvanoforming, and plastic moulding (LIGA process)", Microelectronic Engineering, Vol. 4 No. 1, pp. 35-56

[15] Ahn C-W, Song H-C, Nahm S, Priya S, Park S-H, Uchino K, et al. Effect of ZnO and CuO on the sintering temperature and piezoelectric properties of a hard piezoelctric cermic. J Am Ceram Soc 2006;89(3):921–5. http://dx.doi.org/10.1111/j.1551-2916.2005.00823.x

[16] Etter, P.C. Underwater Acoustic Modeling and Simulation; CRC Press: Boca Raton, FL, USA, 2018.

[17] Sac, H.; Leblebicioğlu, K.; Bozdaği Akar, G. 2D high-frequency forward-looking sonar simulator based on continuous surfaces approach. Turk. J. Electr. Eng. Comput. Sci. 2015, 23, 2289.

[18] Ding, R.; Liu, S. Underwater sound propagation for virtual environments. Vis. Comput. 2021, 37, 2797–2807

[19] YC. Chen Sean Wu, et al, "Lump circuit modeling and matching consideration on acoustical transmitters for underwater application" Jnl. Of Marine Sci. and Tech. (2004)